The Geometric Structure of Deformed Nanotubes and the Topological Coordinates

István László*,† and André Rassat‡

Department of Theoretical Physics, Institute of Physics, Budapest University of Technology and Economics,
H-1521 Budapest, Hungary, and Département de Chimie, Ecole Normale Supérieure, 24, rue Lhomond,
F-75231 Paris Cedex 05, France

After summarizing the harmonic approach to topological coordinates and the null space embedding of graphs, three-coordinated tiling of the plane by hexagons, pentagons, and heptagons are presented and used for the construction of tubular, toroidal, and helical carbon structures. Physically realistic 3D geometries are formed from the corresponding adjacency matrices, and the final structure was obtained with the help of Brenner-potential based molecular mechanics methods.

INTRODUCTION

Geometric representation of graphs has a long history.[1,2] In chemistry it happens very often that only the topological arrangement of the atoms is given, but one needs for further investigations the Cartesian coordinates as well. The structure of a molecule, cluster, or other mesoscopic system is given by a graph, and one is looking for a three-dimensional representation. In this chemical graph the atoms are the vertices and the interatomic bonds are the edges. The topological coordinate method[3−6] gives a very useful procedure for tackling this problem for fullerenes. Motivated by the study of the Colin de Verdière number[7] of graph it was found that the null space of the generalized Laplacian provides a planar embedding on the unit sphere.[8] See further references in ref 9.

In recent publications[10−12] we presented a method for calculating topological coordinates of toroidal structures. In the present work we develop this method for topological coordinates of nanotubes. A single-walled nanotube can be generated by identifying two opposite edges of a parallelogram cut from a hexagonal honeycomb lattice of carbon atoms.[13] It is known that the positive Gaussian curvature in the carbon structures arises from the substitution of some hexagons by pentagons and the negative curvature arises from the substitution by heptagons.[14,15] Thus a polyhex carbon nanotube transforms to a deformed nanotube by pentagonal and heptagonal substitution. Here we shall study especially the helical and toroidal deformations. Although both of them are already studied in the literature,[15−24] here we present a general description after summarizing the topological coordinate method for fullerenes and the null space embedding of graphs.

TOPOLOGICAL COORDINATES OF FULLERENES AND THE NULL SPACE REPRESENTATION OF GRAPHS

The term of topological coordinates for fullerenes was introduced by Manolopoulos and Fowler,[3,4] and it was inspired by Stone's work[25] on bonding in transition-metal clusters. Stone considered a spherical cluster, for which the angular part of the wave function was separated from the radial part. The angular part is a solution of

$$\Delta\Psi = -l(l+1)\Psi \tag{1}$$

where

$$\Delta = \frac{1}{\sin\theta}\frac{\partial}{\partial\theta}\sin\theta\frac{\partial}{\partial\theta} + \frac{1}{\sin^2\theta}\frac{\partial^2}{\partial\phi^2} \tag{2}$$

is the Laplace operator in spherical coordinates. The solutions of eq 1 are the $Y_{lm}(\theta,\phi)$ spherical harmonics labeled by integer quantum numbers $l(\geq 0)$ and m ($-l \leq m \leq l$). The cluster was then treated as an assembly of atoms with nuclei arranged on the surface of a sphere. Using linear combination of atomic orbitals (LCAO) Stone found that the wave function for the system can be well approximated by treating the magnitude of the spherical harmonic functions at an atom site as the coefficient in an LCAO molecular orbital. That is if there are n atoms on a sphere of radius r and their positions are described by the spherical coordinates (r,θ_i,ϕ_i), $i = 1, 2,...n$, then

$$\Psi_{lm}^{\sigma} = \sum_i c_i^{lm}\sigma_i = \sum_i Y_{lm}(\theta_i, \phi_i)\sigma_i \tag{3}$$

are the LCAO molecular orbitals. The σ_i atomic orbitals are s orbitals, or they are directed inward to the origin or outward from the origin. In this reasoning Stone supposed further that there was no mixing between orbitals which differ in l or m and that a set of orbitals with a given l shared the same energy. So there is one orbital, the S^{σ}, which is $l = 0$, and the three orbitals with $l = 1$ are the P^{σ} orbitals. The five orbitals with $l = 2$ are the D^{σ} orbitals. By introducing the

$$Y_{lm}^c = 2^{-\frac{1}{2}}[(-1)^m Y_{lm} + Y_{l,-m}] \tag{4}$$

and

$$Y_{lm}^s = 2^{-\frac{1}{2}}i[(-1)^m Y_{lm} - Y_{l,-m}] \tag{5}$$

† Budapest University of Technology and Economics.
‡ Ecole Normale Supérieure.

real forms of the spherical functions,[26] we obtain that for the lowest energy levels S^σ the c_i coefficients are constants and for the 3-fold degenerated $P_x{}^\sigma$, $P_y{}^\sigma$, and $P_z{}^\sigma$ molecular orbitals the $c_i{}^{P_x}$, $c_i{}^{P_y}$, and $c_i{}^{P_z}$ coefficients are the following:

$$c_i^{P_x} = c^P \sin \theta_i \cos \phi_i \tag{6}$$

$$c_i^{P_y} = c^P \sin \theta_i \sin \phi_i \tag{7}$$

and

$$c_i^{P_z} = c^P \cos \theta_i \tag{8}$$

From this construction it follows that the Cartesian coordinates of the atoms in the cluster can be written down as

$$x_i = r \frac{c_i^{P_x}}{c^P} = r \sin \theta_i \cos \phi_i \tag{9}$$

$$y_i = r \frac{c_i^{P_y}}{c^P} = r \sin \theta_i \sin \phi_i \tag{10}$$

and

$$z_i = r \frac{c_i^{P_x}}{c^P} = r \cos \theta_i \tag{11}$$

Manolopoulos and Fowler[3,4] supposed that if the atomic positions of a spherical cluster can give good approximations for the 3-fold degenerated $P_x{}^\sigma$, $P_y{}^\sigma$, and $P_z{}^\sigma$ molecular orbitals then the $P_x{}^\sigma$, $P_y{}^\sigma$, and $P_z{}^\sigma$ molecular orbitals of a spherical cluster can give good approximations for the atomic positions too.

Let the atomic arrangement of a fullerene (spherical cluster) be given by an n-vertex graph $G = (V, E)$ where V is the set of vertices (set of atoms) and E is the set of edges (set of interatomic bonds). Let **A** be the adjacency matrix with elements $A_{ij} = 1$ if i and j are adjacent and $A_{ij} = 0$ otherwise. Let **H** be the Hückel Hamiltonian-matrix with $H_{ii} = \alpha = 0$ and $H_{ij} = -1$ for bonding between atoms i and j and $H_{ij} = 0$ otherwise. From this definition follows that $\mathbf{H} = -\mathbf{A}$. It is assumed further that

$$a_1 > a_2 \geq a_3 \geq \ldots \geq a_n \tag{12}$$

if a_k is the kth eigenvalue of **A** and $\mathbf{c}^k$ is the corresponding eigenvector. It is clear that $\mathbf{c}^k$ is an eigenvector of **H** with eigenvalue $\lambda_k = -a_k$. As in the fullerenes each carbon atom has three neighbors $a_1 = 3$ and $c_i^1 = 1/\sqrt{n}$ ($i = 1, 2, 3,..., n$). This eigenfunction is the S^σ eigenfunction of **H** with eigenvalue $\lambda_1 = -3$. All that remains is to identify the $P^\sigma{}_x$, $P^\sigma{}_y$, and $P^\sigma{}_z$ eigenvectors of **H** (of **A**).

For any subset U of V let $G| U$ denote the subgraph of G induced by U. (That is $G| U = (U, E')$, where $E' = $ all the edges of G that join two vertices in U.) For any vector **c** let $supp(\mathbf{c})$ denote the support of **c**, that is $supp(\mathbf{c}): = \{i| c_i \neq 0\}$. Furthermore, we denote $supp^+(\mathbf{c}): = \{i| c_i > 0\}$ and $supp^-(\mathbf{c}): = \{i| c_i < 0\}$. The vector **c** is bilobal if $supp(\mathbf{c})$ has exactly two connected components $supp^+(\mathbf{c})$ and $supp^-(\mathbf{c})$.

If $\mathbf{c}^{k_1}$, $\mathbf{c}^{k_2}$, and $\mathbf{c}^{k_3}$ are the first three bilobal eigenfunctions of A or H than Manolopoulos and Fowler introduced the x_i,

y_i, and z_i topological coordinates of the carbon atoms in a fullerene as

$$x_i = S_1 c_i^{k_1} \tag{13}$$

$$y_i = S_2 c_i^{k_2} \tag{14}$$

and

$$z_i = S_3 c_i^{k_3} \tag{15}$$

where $S_\alpha = 1$ or $S_\alpha = 1/\sqrt{(a_1 - a_{k_\alpha})}$ or any other appropriate scaling factors.

It was found for the vast majority of fullerenes that $k_1 = 2$, $k_2 = 3$, and $k_3 = 4$. There are also exceptions such as the C_{60} isomer of D_2 symmetry with $k_1 = 2$, $k_2 = 4$, and $k_3 = 5$.

Now let us turn to the null space representation of graphs.[8] This representation was motivated by the study of the $\mu(G)$ Colin de Verdière parameter[7] of the graph G. Let $G = (V, E)$ be an undirected graph, assuming that $V = \{1,...,n\}$. Then $\mu(G)$ is the largest corank (the multiplicity of the $\lambda = 0$ eigenvalue) of any symmetric matrices $\mathbf{M} = (M_{ij}) \in \mathbf{R}^{(n)}$ such that: (M1). For all i, j with $i \neq j$; $M_{ij} < 0$ if i and j are adjacent, and $M_{ij} = 0$ if i and j are nonadjacent; (M2). **M** has exactly one negative eigenvalue, of multiplicity 1; (M3). There is no nonzero matrix $\mathbf{X} = (X_{ij}) \in \mathbf{R}^{(n)}$ such that $\mathbf{MX} = 0$ and such that $X_{ij} = 0$ whenever $i = j$ or $M_{ij} \neq 0$.

There is no condition on the diagonal entries M_{ii} and the condition (M3) is called the Strong Arnold Property or the Strong Arnold Hypothesis. Condition (M1) means shortly that the real symmetric matrix **M** is the shifted and negatively weighted adjacency matrix of graph G. Thus the Colin de Verdière parameter $\mu(G)$ is the largest multiplicity of the second eigenvalue of the shifted and negatively weighted adjacency matrix if it satisfies the Strong Arnold Condition. The other name of matrix **M** satisfying condition (M1) is generalized Laplacian.[2] We say further that a vector $\mathbf{x} \in ker(\mathbf{M})$ has minimal support if **x** is nonzero and for each nonzero vector $\mathbf{y} \in ker(\mathbf{M})$ with $supp(\mathbf{y}) \subseteq supp(\mathbf{x})$ one has $supp(\mathbf{y}) = supp(\mathbf{x})$.

Lovász and Schrijver proved the following theorem.

Theorem [Lovász and Schrijver[8]]. Let $G = (V, E)$ be a 3-connected planar graph, with $V = \{1,..., n\}$. Let $\mathbf{M} = M_{ij}$ be a symmetric $n \times n$ matrix with exactly one negative eigenvalue (of multiplicity 1), such that for i, j with $i \neq j$, if i and j are adjacent then $M_{ij} \leq 0$ and if i and j are nonadjacent $M_{ij} = 0$, and such that **M** has corank 3. Then the null space $ker\mathbf{M}$ of **M** gives an embedding of G in the sphere S^2 as follows: Let **a**, **b**, and **c** be a basis of $ker\mathbf{M}$, and for $i \in V$ let $\Phi(i): = (a_i, b_i, c_i)$; then $\Phi(i) \neq 0$, and $\Psi(i): = \Phi(i)/||\Phi(i)||$ embeds V in S^2 such that connecting, for any two adjacent vertices i, j, the points $\Psi(i)$ and $\Psi(j)$ by a shortest geodesic on S^2, gives a proper embedding of G in S^2.

In the proof of this theorem results were used from,[9,27] which are related to nodal domain theorems.[28] Roughly speaking, in the null space representation the multiplicity of the second eigenvalue of the negatively weighted adjacency matrix **M** is maximal (=3) and the basis vectors of $ker\mathbf{M}$ are mostly bilobal. If $\mathbf{x} \in ker(\mathbf{M})$ is not bilobal, there is always a bilobal basis vector $\mathbf{y} \in ker(\mathbf{M})$ with $G|supp(\mathbf{y}) \subseteq G|supp(\mathbf{x})$. The topological coordinate method uses directly the first three bilobal eigenvectors of the Hückel Hamiltonian $\mathbf{H} = -\mathbf{A}$.
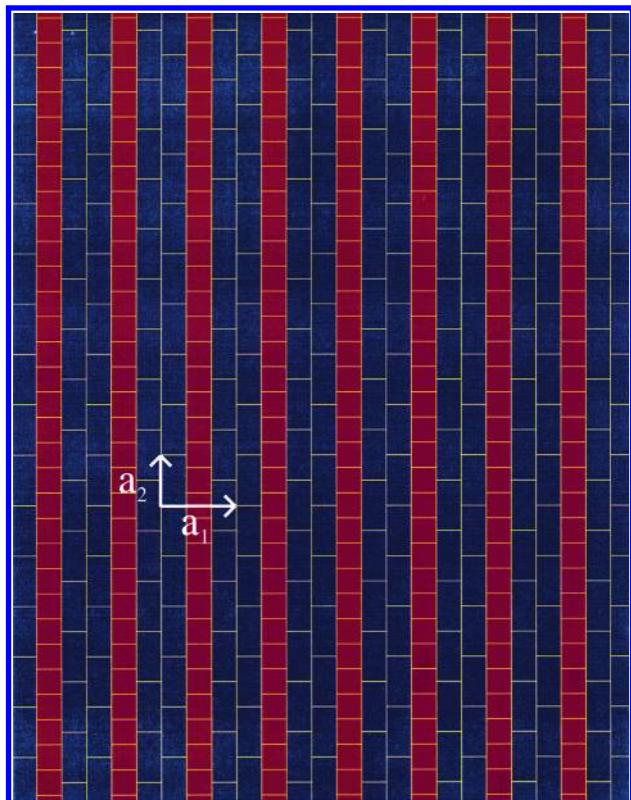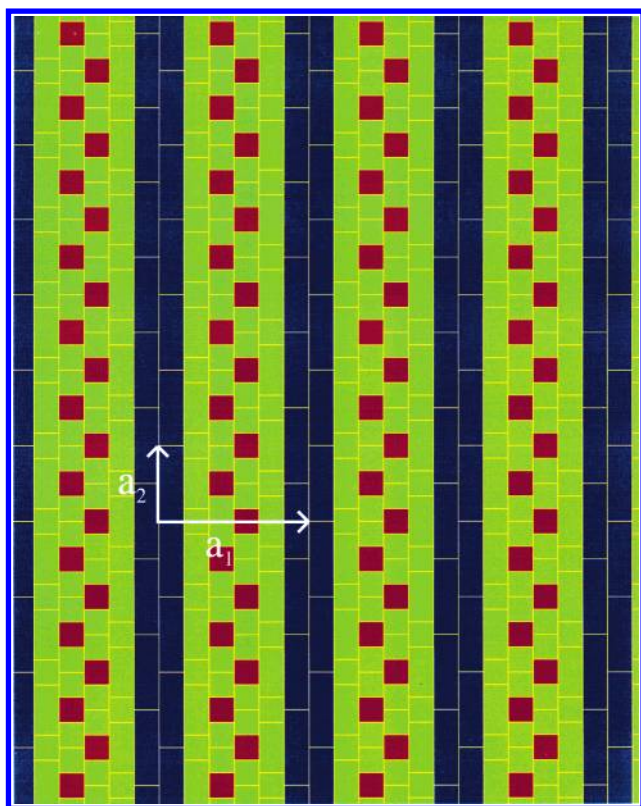
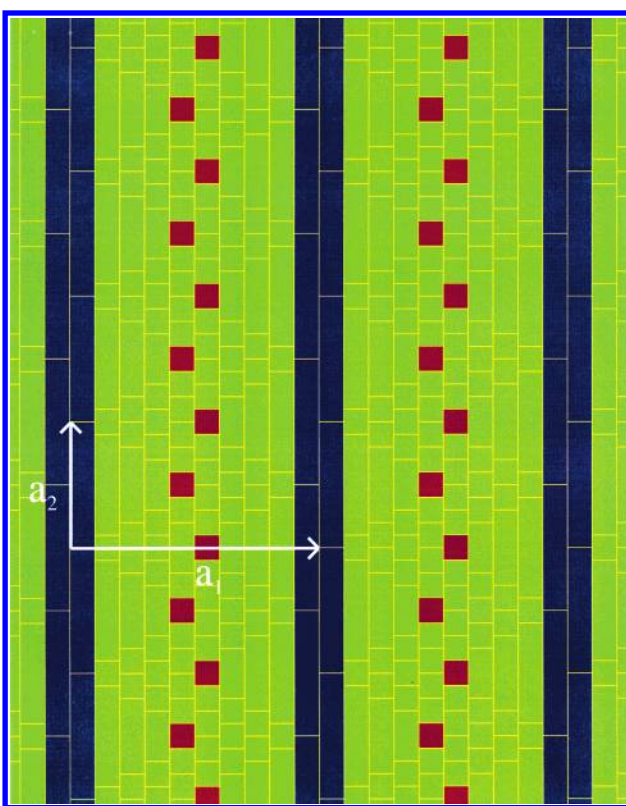**Figure 1.** Tiling of the plane by heptagons and pentagons. $|\mathbf{a_1}| = n_c = 3$, and $l = 1$.
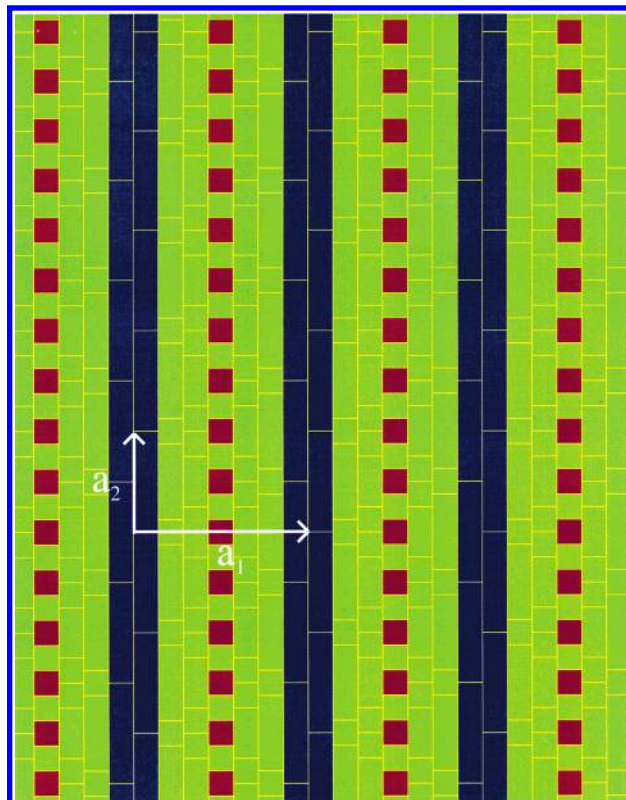
Figure 3. Tiling of the plane by heptagons, hexagons, and pentagons. $|\mathbf{a_1}| = n_c = 7$, and $l = 3$.

Figure 2. Tiling of the plane by heptagons, hexagons, and pentagons. $|\mathbf{a_1}| = n_c = 6$, and $l = 2$.

**Figure 4.** Tiling of the plane by heptagons, hexagons, and pentagons. $|\mathbf{a_1}| = n_c = 10$, and $l = 4$.

As the corank of $\mathbf{H} \leq 3$ they represent the basis vectors of *ker*$\mathbf{M}$ after splitting up the second eigenvalue of $\mathbf{M}$.

Topological Coordinates of Tori and Nanotubes. In refs 11 and 12 a method was presented for topological coordinates of toroidal carbon structures. Let us suppose that the

topological structure of the torus is given by the $G = (V, E)$ graph. Let $\mathbf{A}$ be the corresponding adjacency matrix and $\mathbf{H} = -\mathbf{A}$ be the Hückel Hamiltonian-matrix. As before let c^k be the kth eigenfunction of $\mathbf{H}$ (of $\mathbf{A}$) and λ_k ($a_k = -\lambda_k$) be the corresponding eigenvalue. We chose four bilobal eigen-
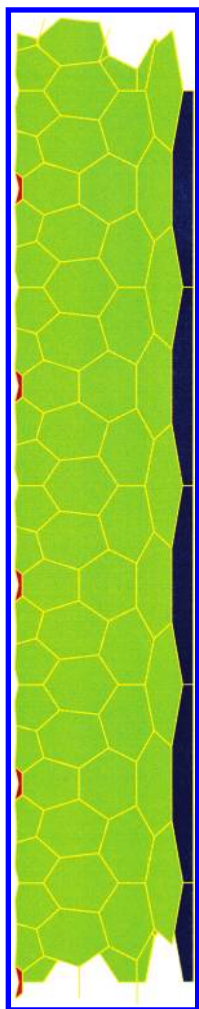
Figure 5. Nanotube having the topological coordinates obtained from parameters (4, 1, 0, 0, 5). The tiling is in Figure 4. with super cell vectors $\mathbf{b_1} = \mathbf{a_1}$ and $\mathbf{b_2} = 5\mathbf{a_2}$.

vectors $\mathbf{c}^{k_1}$, $\mathbf{c}^{k_2}$, $\mathbf{c}^{k_3}$, and $\mathbf{c}^{k_4}$, and the topological coordinates of the torus are calculated as

$$x_i = S_1 C_i^{k_1}(1 + S_4 C_i^{k_4}) \tag{16}$$

$$y_i = S_2 C_i^{k_2}(1 + S_4 C_i^{k_4}) \tag{17}$$

$$z_i = S_3 C_i^{k_3} \tag{18}$$

where S_1, S_2, S_3, and S_4 appropriate scaling factors as before. Concerning difficulties using only three bilobal eigenvectors for the torus see ref 10.

In this formula the position of the point i is the sum of a vector $\mathbf{R}_i = \mathbf{R}_i(\mathbf{c}_i^{k_1}, \mathbf{c}_i^{k_2})$ directed from the center of gravity of the torus to a point on the circular spine and a vector $\mathbf{r}_i = \mathbf{r}_i(\mathbf{c}_i^{k_3}, \mathbf{c}_i^{k_4})$. If the radial vectors $\mathbf{R}_i = \mathbf{R}_i(\mathbf{c}_i^{k_1}, \mathbf{c}_i^{k_2})$ and $\mathbf{r}_i = \mathbf{r}_i(\mathbf{c}_i^{k_3}, \mathbf{c}_i^{k_4})$ give a proper embedding of the graph in the surface of the torus, then the radial vectors $\mathbf{R}_i = \mathbf{R}_i(\mathbf{c}_i^{k_3}, \mathbf{c}_i^{k_4})$ and $\mathbf{r}_i = \mathbf{r}_i(\mathbf{c}_i^{k_1}, \mathbf{c}_i^{k_2})$ give a proper embedding too, but usually the radial vectors $\mathbf{R}_i = \mathbf{R}_i(\mathbf{c}_i^{k_1}, \mathbf{c}_i^{k_3})$ and $\mathbf{r}_i = \mathbf{r}_i(\mathbf{c}_i^{k_2}, \mathbf{c}_i^{k_4})$ give an improper embedding. These results show that the pairs of eigenvectors $(\mathbf{c}^{k_1}, \mathbf{c}^{k_2})$ and $(\mathbf{c}^{k_3}, \mathbf{c}^{k_4})$ might be the corresponding eigenvectors of two 2-fold degenerated eigenvalues of a matrix M defined in a similar way as in the case of the null space embedding of planar graphs.
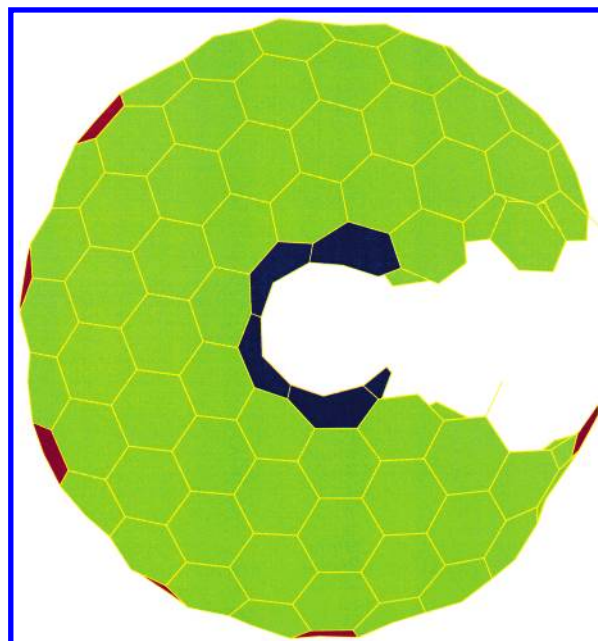
Figure 6. The final structure after molecular mechanical relaxation of the topological coordinates of Figure 5 is a toroidal structure.

As our purpose is to find appropriate Cartesian coordinates we scaled the $\mathbf{R}_i$, $\mathbf{r}_i$ position vectors individually in order to obtain the relations $R = |\mathbf{R}_i|$ and $r = |\mathbf{r}_i|$ by taking the average values of $|\mathbf{R}_i|$ and $|\mathbf{r}_i|$ and not changing the directions. By introducing the ϕ_i azimuthal angles between the X axis and the direction of the vectors $\mathbf{R}_i$ we can write $\mathbf{R}_i = (R\cos\phi_i, R\sin\phi_i)$. With the help of the angles ϕ_i the torus can be transformed into a nanotube by the relations $x_i = S_3 \mathbf{c}_i^{k_3}$, $y_i = S_3 \mathbf{c}_i^{k_4}$, and $z_i = R\phi_i$. That is the topological coordinates of a nanotube obtained from the torus are the following:

$$x_i = S_3 C_i^{k_3} \tag{19}$$

$$y_i = S_4 C_i^{k_4} \tag{20}$$

$$z_i = R \arccos(S_1 C_i^{k_1}/R) \quad if\ C_i^{k_2} \geq 0 \tag{21}$$

and

$$z_i = R(2\pi - \arccos(S_1 C_i^{k_1}/R)) \quad if\ C_i^{k_2} < 0 \tag{22}$$

A similar formula can be written down if we define the origin of the angles ϕ_i at an angle α measured from the direction of the X axis in the torus.

RESULTS

The $G = (V, E)$ graph of a polyhex carbon nanotube and a polyhex carbon torus can be obtained from a hexagonal graphite sheet generated from two unit cell vectors $\mathbf{a_1} = a(\sqrt{3}/2, 1/2)$ and $\mathbf{a_2} = a(\sqrt{3}/2, -1/2)$.[22] Each unit cell contain two atoms at positions $(0, 0)$ and $(a, 0)$. Then a parallelogram is constructed from the vectors $\mathbf{b_1} = n\mathbf{a_1} + m\mathbf{a_2}$ and $\mathbf{b_2} = p\mathbf{a_1} + q\mathbf{a_2}$, where n, m, p, and q are integers. We shall call this parallelogram super cell. The graph G of the nanotube is obtained by identifying two opposite edges of the parallelogram, and identification of each pair of opposite edges yields the graph G of a torus. It is known
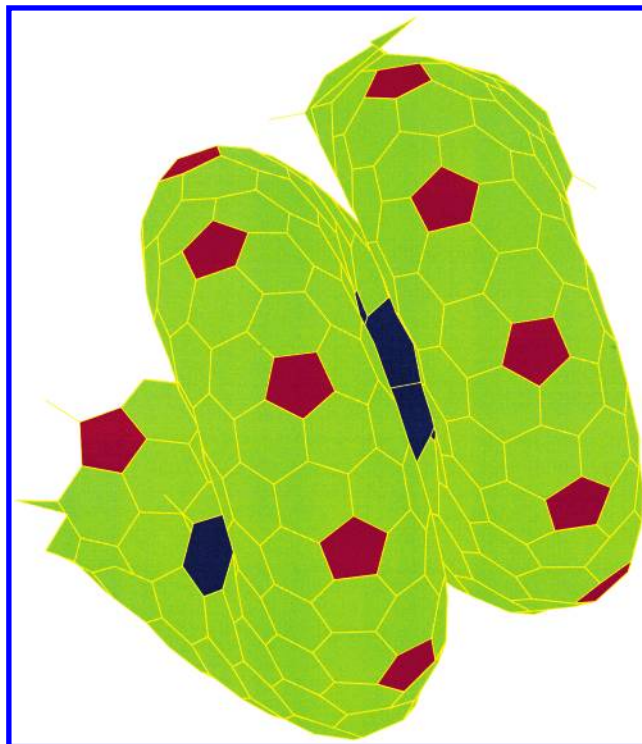
GEOMETRIC STRUCTURE OF DEFORMED NANOTUBES

J. Chem. Inf. Comput. Sci., Vol. 43, No. 2, 2003 **523**

Figure 7. Nanotube having the topological coordinates obtained from parameters (4, 1, −1, 5, 5). The tiling is in Figure 4 with super cell vectors $\mathbf{b_1} = \mathbf{a_1} - \mathbf{a_2}$ and $\mathbf{b_2} = 5\mathbf{a_1} + 5\mathbf{a_2}$.

Figure 8. The final structure after molecular mechanical relaxation of the topological coordinates of Figure 7 is a helical structure.

that the pentagonal defects in the polyhex planar graphite sheet produce positive Gaussian curvature and that the effect of heptagonal defects can be negative curvature.[14,15]

In Figures 1−4 periodic tilings are shown containing hexagonal pentagonal and heptagonal faces. As for the graph $G = (V, E)$ we need only the topological structure; the lattices are presented in a stylized form after Kirby.[29] The unit-cells are determined by the horizontal vector $\mathbf{a_1}$ and vertical vector $\mathbf{a_2}$. The heptagons and pentagons are placed in vertical columns. The $|\mathbf{a_2}|$ length of $\mathbf{a_2}$ is equal to the distance between two horizontal lines in the column of heptagons and $|\mathbf{a_1}| = n_c$, where n_c equals to the number of vertical columns

in the unit-cell. If the unit-cells are marked by the positive integers $l = 1, 2,...$, then $n_c = (l - 1)2 + 3$ if l is even number and $n_c = (l - 1)2 + 4$ if l is odd number. As in the case of polyhex lattice we can define the super cell parallelogram by the vectors $\mathbf{b_1} = n\mathbf{a_1} + m\mathbf{a_2}$ and $\mathbf{b_2} = p\mathbf{a_1} + q\mathbf{a_2}$, where n, m, p, and q are integers. Identification of the opposite edges gives the graph $G = (V, E)$ of the parameters (l, n, m, p, q). Figure 5 shows the nanotube with the parameters (4, 1, 0, 0, 5) and calculated by the eqs 19−22. Thus the lattice of Figure 4 was used, with the super cell vectors $\mathbf{b_1} = \mathbf{a_1}$ and $\mathbf{b_2} = 5\mathbf{a_2}$. The vectors $\mathbf{b_1}$ and $\mathbf{b_2}$ are perpendicular to each other, and $\mathbf{b_2}$ is parallel with the lines of heptagons and pentagons. After obtaining the topological coordinates for a given super cell of parameters (l, n, m, p, q) in a tiling, the final structure was reached with the help of a molecular mechanics method based on the Brenner potential.[30] In this relaxation process we supposed interactions only between the first neighbors determined by the unit-cells of the tiling. From the topological coordinates of Figure 5 we obtained the toroidal structure of Figure 6. In this open torus the pentagons are at the places of positive Gaussian curvatures, and the heptagons are found at the negative Gaussian curvatures.

Let us see what happens if we chose the super cell of parameters (4, 1, −1, 5, 5) with the tiling of Figure 4 and with super cell vectors $\mathbf{b_1} = \mathbf{a_1} - \mathbf{a_2}$ and $\mathbf{b_2} = 5\mathbf{a_1} + 5\mathbf{a_2}$. Now $\mathbf{b_2}$ is not parallel with the lines of pentagons and heptagons, but it is perpendicular to $\mathbf{b_1}$. Figures 7 and 8 show the structures obtained before and after optimization, respectively. As the vector $\mathbf{b_2}$ is not parallel with the lines of pentagons and heptagons, we obtained a helical structure. If the graph $G = (V, E)$ is constructed from a purely polyhex tiling, the relaxed structures always remain nanotube as there are not pentagons and heptagons that are necessary for positive and negative Gaussian curvatures.

524 *J. Chem. Inf. Comput. Sci., Vol. 43, No. 2, 2003*

LÁSZLÓ AND RASSAT

In conclusion we can say that using a given periodic tiling by hexagons pentagons and heptagons, the final relaxed structure depends on the tiling and on the particular position of the super cell.

REFERENCES AND NOTES

(1) Lovász, L.; Vesztergombi, K. Geometric Representations of Graphs. In *Paul Erdös and his Mathematics*; Halász, L., Lovász, L., Simonovits, M. T., Sós, V., Eds.; Bolyai Society − Springer-Verlag: 1999.

(2) Godsil, Ch.; Royle, G. *Algebraic Graph Theory*; Springer-Verlag: New York, Berlin, Heidelberg, 2001; Chapter 13.

(3) Manolopoulos D. E.; Fowler, P. W. Molecular Graphs, Point Groups, and Fullerenes. *J. Chem. Phys.* **1992**, *96*, 7603−7614.

(4) Fowler, P. W.; Manolopoulos D. E. *An Atlas of Fullerenes*; Clarendon Press: Oxford, 1995; Chapter 5, pp 101−104.

(5) Fowler, P. W.; Pisanski, T.; Shawe-Taylor, J. Molecular graph eigenvectors for molecular coordinates. In *Graph drawing: DIMACS international workshop. GD'94, Princeton, New Jersey, USA, October 10−12, 1994: proceedings*; (Lecture notes in computer science, 894). Tamassia, R., Ed.; Springer-Verlag: Berlin, 1995; pp 282−285.

(6) Pisanski, J.; Shawe-Taylor, J. Characterizing graph drawings with eigenvectors. *J. Chem. Inf. Comput. Sci.* **2000**, *40*, 567−471.

(7) Colin de Verdière, Y. Sur un nouvel invariant des graphes et un critère de planarité. *Combinatorial Theory, Ser. B* **1990**, *50*, 11−21.

(8) Lovász, L.; Schrijver, A. On the Null Space of a Colin de Verdière Matrix. *Annales de l'Institute Fourier (Grenoble)* **1999**, *49*, 1017−1026.

(9) van der Holst, H.; Lovász, L.; Schrijver, A. The Colin de Verdière Graph Parameter. In *Graph Theory and Combinatorial Biology (Balatonlelle, 1999)*; Bolyai Society: Budapest, 1999; pp 29−85.

(10) Graovac, A.; Plavšić, D.; Kaufman, M.; Pisanski, T.; Kirby, E. C. Application of the Adjacency Matrix Eigenvectors Method to Geometry Determination of Toroidal Carbon Molecules. *J. Chem. Phys.* **2000**, *113*, 1925−1931.

(11) László, I.; Rassat, A.; Fowler, P. W.; Graovac, A. Topological Coordinates for Toroidal Structures. *Chem. Phys. Lett.* **2001**, *342*, 369−374.

(12) László, I.; Rassat, A.; Fowler, P. W.; Graovac, A. Topological coordinates for carbon nanostructures. In *Electronic Properties of Novel Materials, XV International Winterschool, Kirchberg, Austria 2001*; Kuzmany, H., Fink, J., Mehring, M., Roth, S., Eds.; The American Institute of Physics Conference Proceedings: Melville, NY, 2001; pp 438−441.

(13) Dresselhaus, M. S.; Dresselhaus, G.; Eklund, P. C. *Science of Fullerenes and Carbon Nanotubes*; Academic Press: San Diego, Boston, New York, London, Sydney, Tokyo, Toronto, 1996; Chapter 19.

(14) Mackay, A. L.; Terrones, H. Diamond from graphite. *Nature* **1991**, *352*, 762.

(15) Ihara, S.; Itoh, S.; Kitakami, J.-i. Toroidal Forms of Graphitic Carbon. *Phys. Rev. B* **1993**, *47*, 12908−12911.

(16) Ihara, S.; Itoh, S.; Kitakami, J.-i. Helically Coiled Cage Forms of Graphitic Carbon. *Phys. Rev. B* **1993**, *48*, 5643−5647.

(17) Itoh, S.; Ihara, S. Toroidal Forms of Graphitic Carbon. II. Elongated Tori. *Phys. Rev. B* **1993**, *48*, 8323−8328.

(18) Amelinckx, S.; Zhang, X. B.; Bernaerts, D.; Zhang, X. F.; Ivanov, V.; Nagy, J. B. A Formation Mechanism for Catalytically Grown Helix-shaped Graphite Nanotubes. *Science* **1994**, *265*, 635−639.

(19) Akagi, K.; Tamura, R.; Tsukada, M.; Itoh, S.; Ihara, S. Electronic Structure of Helically Coiled Cage of Graphitic Carbon. *Phys. Rev. Lett.* **1995**, *74*, 2307−2310.

(20) Akagi, K.; Tamura, R.; Tsukada, M.; Itoh, S.; Ihara, S. Electronic Structure of Helically Coiled Carbon Nanotubes: Relation Between the Phason Lines and Energy Band Features. *Phys. Rev. B* **1996**, *53*, 2114−2120.

(21) Volodin, A.; Ahlskog, E.; Seynaeve, E.; van Haesendonck, C. Imaging the Elastic Properties of Coiled Carbon Nanotubes with Atomic Force Microscopy. *Phys. Rev. Lett.* **2000**, *84*, 3342−3345.

(22) Ceulemans, A.; Chibotaru, L. F.; Bovin, S. A.; Fowler, P. W. The Electronic Structure of Polyhex Carbon Tori. *J. Chem. Phys.* **2000**, *112*, 4271−4278.

(23) Bíró, L. P.; Lazarescu, S. D.; Thiry, P. A.; Fonseca, A.; Nagy, J. B.; Lucas, A. A.; Lambin, Ph. Scanning Tunneling Microscopy Observation of Tightly Wound, Single-wall Coiled Carbon Nanotubes. *Europhys. Lett.* **2000**, *50*, 494−500.

(24) László, I.; Rassat, A. Toroidal and Spherical Fullerene-like Molecules with Only Pentagonal and Heptagonal Faces. *Int. J. Quantum Chem.* **2001**, *84*, 136−139.

(25) Stone, A. J. New Approach to Bonding in Transition-Metal Clusters and Related Compounds. *Inorg. Chem.* **1981**, *20*, 563−571.

(26) Grifith, J. S. *The Theory of Transition Metal Ions*; Cambridge University Press: London, 1961; p 166.

(27) van der Holst, H. *Topological and Spectral Graph Characterizations*, Ph.D. Thesis, University of Amsterdam, Amsterdam, 1996.

(28) Gladwell, G. M. L.; Davies, E. B.; Leydold, J.; Stadler, P. F. Discrete nodal domain theorems. *Lin. Alg. Appl.* **2001**, *336*, 51−60.

(29) Kirby, E. C. On Toroidal Azulenoids and Other Shapes of Fullerene Cage *Fullerene Sci. Technol.* **1994**, *2*, 395−404.

(30) Brenner, D. W. Empirical Potentials for Hydrocarbons for Use in Simulating the Chemical Vapor Deposition of Diamond Films. *Phys. Rev. B* **1990**, *42*, 9458−9471.